Local Binary Pattern Statistics Feature for Reduced Reference Image Quality Assessment

Min Zhang*[a], Xuanqin Mou[b], Hiroshi Fujita[a], Lei Zhang[c], Xiangrong Zhou[a] and Wufeng Xue[b,c]

[a]Department of Intelligent Image Information, Division of Regeneration and Advanced Medical Sciences, Graduate School of Medicine, Gifu University, Gifu-shi, 501-1194 Japan
[b]Institute of Image Processing and Pattern Recognition, Xi'an Jiaotong University, China
[c]Department of Computing, Hong Kong Polytechnic University, Hung Hom, Kowloon, Hong Kong

ABSTRACT

Measurement of visual quality is of fundamental importance for numerous image and video processing applications. This paper presented a novel and concise reduced reference (RR) image quality assessment method. Statistics of local binary pattern (LBP) is introduced as a similarity measure to form a novel RR image quality assessment (IQA) method for the first time. With this method, first, the test image is decomposed with a multi-scale transform. Second, LBP encoding maps are extracted for each of subband images. Third, the histograms are extracted from the LBP encoding map to form the RR features. In this way, image structure primitive information for RR features extraction can be reduced greatly. Hence, new RR IQA method is formed with only at most 56 RR features. The experimental results on two large scale IQA databases show that the statistic of LBPs is fairly robust and reliable to RR IQA task. The proposed methods show strong correlations with subjective quality evaluations.

Keywords: Image quality assessment (IQA), reduced reference, local binary pattern.

1. INTRODUCTION

In recent years, image quality assessment (IQA) has been attracting much research attention because of its importance in various image/video processing applications. With these IQA methods, human behaviors can be automatically predicted in evaluating image quality. Depending on the availability of a reference image, IQA methods can be divided into three categories: full-reference (FR, where the reference image is fully available when evaluating the perceptual quality of the distorted image), reduced-reference (RR, where only partial information about the reference image is available), and no-reference (NR, where no access to the reference image is allowed).

FR models have been investigated for a long time. Conventional FR IQA indices such as mean squared error (MSE) and peak signal-to-noise ratio (PSNR) have been used for a long time but they do not conform well to the human visual perception. In the last decade, much effort and progress have been made on FR IQA and their performance has been validated across existed distortion types in realistic world. Some FR methods are based on known models of bottom-up human visual system (HVS) [1-3]. Some are based on overarching principles of what the HVS is trying to accomplish when viewing a distorted image, such as Structural SIMilarity index (SSIM) [4] and NSER [5]. Some are motivated by the natural scene statistics (NSS) and they use the information fidelity criteria to quantify the information shared between the distorted and the reference images [6, 7].

However, in most practical scenarios where the reference image is not available, the application of FR IQA models will be restricted greatly. In these cases, either NR or RR IQA models are required. Given NR IQA being an extremely difficult task so far, RR methods are considered as the compromise between the unfeasibility of FR models and unavailability of NR models. It becomes more and more attractive because of its flexibility and practicability in real-world applications, such as image and video transmission. RR IQA methods development is still in progress and much desired [8].

*min@fjt.info.gifu-u.ac.jp; zhangmin@mailst.xjtu.edu.cn

Digital Photography IX, edited by Nitin Sampat, Sebastiano Battiato, Proc. of SPIE-IS&T Electronic Imaging,
SPIE Vol. 8660, 86600L · © 2013 SPIE-IS&T · CCC code: 0277-786/13/$18 · doi: 10.1117/12.2008646

RR IQA method is designed to predict the perceptual quality of distorted images with only partial information about the reference images. Certainly, the RR feature extraction is absolutely of most significance in RR metric. For example, Zhou Wang et al. proposed the concept of quality aware images in [9], where partial reference image information is embedded within the image and can be extracted reliably despite distortions for the first time. After that, a lot of relevant progress has been made in this area [9-15]. Some RR IQA works favor the natural scene statistic (NSS) based RR feature extraction. NSS based feature extraction provides a highly efficient way to summarize the image information, and lead to RR IQA algorithms with low RR data rate [9]. Moreover, the statistics of image basic primitives, such as edge and gradient magnitude are also utilized for developing RR IQA models [10, 11, 15]. Meanwhile there are some RR IQA methods taking into account the visual sensitivity before feature extraction in some transformation domain. In [12], the CSF filter was applied in the contourlet domain or the wavelet domain to determine the visual threshold. Recently, there is another noticeable trend to estimate RR IQA models from the state of the art FR IQA models, such as RR-SSIM method [13], which is reduced information estimation from SSIM index [4], and RRED indices [14], which is estimated from visual information fidelity (VIF) index [7]. These methods are trying to find the relationship between the FR measure and their RR estimation.

As a quite efficient and discriminant local structure descriptor, local binary pattern (LBP) has achieved great success in computer vision and pattern recognition. Although LBP is only the sign component of local image information, it has been proved that LBP preserves much more image local structural information than the magnitude component [20]. The most frequent local binary patterns correspond to primitive local structure, such as edges, corners, and spots; hence, they can be regarded as feature detectors that are triggered by the best matching pattern [16]. From the viewpoint of visual perception, image local structural change could reflect the degradation of image quality and this has been validated by a serious of relevant IQA works, such as SSIM Index mentioned above [4], and Non-Shift Edge Ratio (NSER) [5], etc. Since LBP is quite efficient in the presentation of image local structures, in this paper, we consider that LBP encoding map of images could serve as a novel IQA index potentially. Quality concerned information of the image can be easily refined greatly in the form of the histogram of the LBP code. With the RR feature formed by the LBP histograms, high performance novel RR IQA method is expected.

The rest of the paper is organized as follows. Section 2 presents the proposed reduced reference metric. Section 3 details the experimental setup. Section 4 presents the experimental results and discussions. Section 5 concludes the paper.

2. THE PROPOSED METHOD

2.1 An Overview of Local Binary Pattern (LBP)

Recently, local binary texture patterns termed "uniform" are recognized as the fundamental properties of local image feature [16]. The term "uniform" refers to the uniform appearance of the local binary pattern (LBP).

Formally, the LBP operator takes the form

$$LBP_{P,R} = \sum_{p=0}^{P-1} S(t_i - t_c)2^p, \quad where \quad S(t) = \begin{cases} 1, & t \geq 0 \\ 0, & t < 0 \end{cases}. \tag{1}$$

t_c is the gray value of the central pixel, t_i is the value of its neighbors, P is the total number of involved neighbors and R is the radius of the neighborhood. The gray values of neighbors that are not in the image grids can be estimated by interpolation. At a center pixel t_c, each neighboring pixel t_i is assigned with a binary label, which can be either “0” or “1,” depending on whether the center pixel has higher intensity value than the neighboring pixel (see Fig. 1 for the basic LBP illustration, giving 8 bit integer LBP codes based on the 8 pixels around the central one).

Suppose the image is of size $M \times N$. After the LBP code of each pixel is identified, a histogram is built to represent the image:

$$\begin{aligned} H(i) &= \sum_{m=1}^{M} \sum_{n=1}^{N} f(LBP(m,n), i), i \in [0, I], \\ f(x,y) &= \begin{cases} 1, x = y \\ 0, otherwise \end{cases} \end{aligned} \tag{2}$$

In which I is the number of different LBP codes produced by the LBP operator.

The uniform LBP patterns refer to the patterns which has limited transition or discontinuities (bitwise 0/1 changes) in the LBP. The "uniform" patterns is defined as a uniformity measure U ("pattern")

$$U(LBP_{P,R}) = \left|s(t_{P-1}-t_c)\right| + \sum_{p=1}^{P-1}\left|s(t_p-t_c)-s(t_{p-1}-t_c)\right| \tag{3}$$

U value of at most 2 is defined as "uniform" patterns.

To achieve rotation invariance, a locally rotation invariant pattern could be defined as

$$LBP_{P,R}^{riu2} = \begin{cases} \sum_{p=0}^{P-1} S(t_p - t_c) & if \quad U(LBP_{P,R}) \le 2 \\ P+1 & otherwise \end{cases} \tag{4}$$

Superscript ^{riu2} reflects the use of rotation invariant "uniform" patterns that have U value of at most 2.

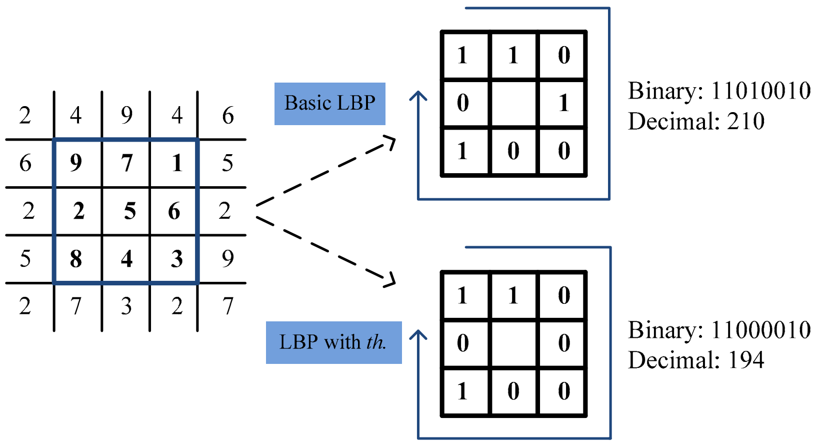

Figure 1 Comparison of the basic LBP code and the LBP code with threshold "2" for the region in the black square.

2.2 The Proposed Reduced Reference Feature Extraction Method

Undoubtedly, the RR feature extraction is of most significance. A successful RR quality assessment method must achieve a good balance between the data rate of RR features and the accuracy of image quality prediction. Since that, the key issue of RR IQA method is how to accurately model the computational relationship between the statistics of the image features and the image degradation degree.

With LBP coding method, the proposed reduced reference image feature extraction scheme is shown in Fig.2.

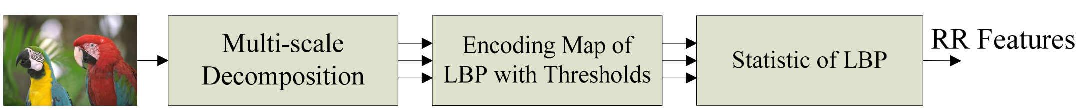

Figure 2 The scheme for the proposed reduced reference feature extraction.

With this proposed method, the detail of RR feature extraction process is as follows.

1) Multi-scale decomposition

From a computational point of view, the response of classical receptive field (CRF) of human visual system (HVS) can be modeled by a series of hierarchical filters, i.e. the Laplacian of Gaussian (LOG) filters, which is defined as

$$\nabla^2 G(r,\sigma) = -\frac{1}{\pi\sigma^4}\left[1-\frac{r^2}{2\sigma^2}\right]\exp\left(-\frac{r^2}{2\sigma^2}\right), \tag{5}$$

where $G(r,\sigma)=\frac{1}{2\pi\sigma^2}\exp\left(-\frac{r^2}{2\sigma^2}\right)$ is the Gaussian kernel and $r^2=x^2+y^2$.

2) Encoding map of LBP with threshold

In practice LBP code is sensitive to random and quantization noise. To counter this, an extended LBP named Local Ternary Pattern (LTP) is proposed with a 3-valued coding that includes a threshold around zero for improved resistance to noise [17]. Concerning IQA, noise under human visual detection threshold also should be avoided in the statistics of LBP codes. But LTP produces more histogram bins, which adds the burden to data rate of RR features. For example, LTP produce $3^4-1=80$ histogram bins and LBP produce $2^4-1=15$ histogram bins when $R=1$ and $P=4$.

For simplicity, in this paper, local binary pattern with thresholds is involved (see Fig. 1 for an illustration). It is defined as

$$LBP_{P,R}=\sum_{p=0}^{P-1}S(t_i-t_c)2^p, \quad where \quad S(t)=\begin{cases}1, & \mathrm{abs}(t)\geq Threshold\\ 0, & \mathrm{abs}(t)<Threshold.\end{cases} \tag{6}$$

In this way, the LBP with threshold produce the same histogram bins as basic LBP while the noise under human visual detection threshold is avoided partly.

3) RR feature extracted from LBP histograms

The histograms from the statistics of LBP codes that record the occurrences of various patterns in the neighborhood of each pixel for every sub-band images are extracted to form the RR features. In this paper, the proposed method is implemented in two ways, including the uniform LBPs and the rotation invariant uniform LBPs [16] respectively.

2.3 Distortion measure

With the proposed method, the RR features for the reference image are extracted at the sender side. It is firstly quantized and transmitted to the receiver side. Then the RR features for the distorted image are extracted at the receiver side in the same way. Several possible similarity measures are available to compute the visual distortion degree between the reference image and the distorted image. In this paper, Kullback-Leibler divergence (KLD) is adopted to compute the distance D_{band} between the RR features P_{band} and Q_{band} of the reference image and the distorted image, for each sub-band images respectively.

$$D_{band}=\sum_{i=1}^{N}P_{band}(i)\log\frac{P_{band}(i)}{Q_{band}(i)} \tag{7}$$

N is the number of decomposition scales.

Finally, the overall perceptual distortion of the received image is computed as the sum of the distortion measures of all subbands

$$D_{band}=\sum_{All\ \ Subbands}\log(D_{band}) \tag{8}$$

3. EXPERIMENTAL SETUP

3.1 Databases for evaluation

To validate the proposed RR IQA algorithm, two large scale publicly available subject-rated image databases are used, which are the LIVE database [18] developed at laboratory for image and video engineering at the university of Texas at Austin and the Categorical Subjective Image Quality (CSIQ) database [19] developed at computational perception and image quality laboratory at Oklahoma State University.

- The LIVE database contains seven datasets of 982 subject-rated images created from 29 original images with five types of distortions at different distortion levels. The distortion types include 1) JP2:JPEG2000 compression, 2) JPEG: JPEG compression, 3) Noise: white noise contamination, 4) Blur: Gaussian blur and 5) FF: fast fading channel distortion of JPEG2000 compressed bitstream. The subjective test was carried out with each of the five data sets individually.

- The Categorical Subjective Image Quality (CSIQ) database contains 866 distorted images, including six types of distortions at three to five distortion levels. The distortion types include baseline JPEG compression, JPEG2000 compression, global contrast decrements, additive pink Gaussian noise, Gaussian blurring and additive Gaussian white noise.

3.2 Performance evaluation methods

The spearman rank order correlation coefficient (SROCC), the linear correlation coefficient (CC) and the root mean square error (RMSE) between the objective scores predicted by the computational model and the subjective scores predicted by observers after nonlinear regression are used to evaluate the performance of these IQA methods. Higher SROCC, CC and lower RMSE indicate better consistency with human perceptual distortion degree. According to the VQEG Phase-II report [16], a five-parameter nonlinear function mapping between the objective score and the subjective scores is allowed to transform the objective score to the predicted quality value. The mapping function is defined as follow [16]:

$$\mathrm{Quality}(x)=\beta_1\left(\frac{1}{2}-\frac{1}{1+\exp(\beta_2(x-\beta_3))}\right)+\beta_4 x+\beta_5. \tag{9}$$

3.3 Implementation details

The proposed algorithm is compared with 5 state-of-the-art RR IQA metrics, including the method in [9], the method in [10], the method in [11], the method in [13] and the method in [15]. PSNR is also included. All of them work on the luminance component only.

For the proposed algorithm, the test image is decomposed into 4 scales. For each scale, the LBP codes are computed with different R and P. In this paper, $R=1$ and $P=4$ are selected. The number of features are 14 and 5 for the uniform LBPs (indicated as RR-LBPS$_{P,R}^{u2}$) and rotation invariant uniform LBPs (indicated as RR-LBPS$_{P,R}^{riu2}$) of each scale, respectively. The total numbers of RR features are correspondingly 56 and 20 when the number of decomposition scales is 4. The thresholds of LBP for the 4 decomposition scales are [0.6 4.8 0 0.5]. In this study, we need not apply any extra training on the database.

4. EXPERIMENTAL RESULTS AND DISCUSSION

Under the reduced reference feature extraction scheme shown in Fig.2, preliminary experiments are carried out. To provide a quantitative measure, the experimental results for RR IQA methods performance comparison on LIVE database are demonstrated in Table 1, Table 2 and Table 3. Table 4 shows the preliminary results comparison evaluated on the CSIQ IQA database. The best three results for each distortion type and each database are highlighted in bold. Table 1 shows the CC, SROCC and RMSE results of the proposed methods on the LIVE IQA database. Table 2 and Table 3 compare both the performance of overall prediction accuracy and the specific distortion prediction accuracy of the proposed methods with that of the competitive RR IQA methods, as well as PSNR. 'No. of scalars' indicates the amount of information required from the reference for quality computation.

TABLE 1: PERFORMANCE OF THE PROPOSED METHODS ON LIVE IMAGE QUALITY DATABASE.

Model/Distortion		JP2	JPEG	Noise	Blur	FF	Overall	No. of scalars
RR-LBPS$_{P,R}^{u2}$	SROCC	0.9561	0.9555	0.9594	0.9581	0.9582	0.9186	56
	CC	0.9638	0.9585	0.9632	0.9650	0.9572	0.9127	
	RMSE	6.7274	9.0804	7.5247	4.8433	8.2457	8.2457	
RR-LBPS$_{P,R}^{riu2}$	SROCC	0.9511	0.9525	0.9613	0.9511	0.9583	0.9127	20
	CC	0.9566	0.9579	0.9638	0.9594	0.9573	0.9082	
	RMSE	7.3530	9.1440	7.4619	5.2118	8.2350	11.4380	

Table 2: Experimental results of SROCC for the proposed method and the state of the art RR and PSNR, evaluated by LIVE database.

Model/Distortion	JP2(1)	JP2(2)	JPEG(1)	JPEG(2)	Noise	Blur	FF	Overall	No. of scalars
RR-LBPS$_{P,R}^{u2}$	**0.9670**	**0.9661**	**0.9150**	0.8929	0.9594	**0.9581**	**0.9582**	**0.9186**	56
RR-LBPS$_{P,R}^{riu2}$	**0.9565**	**0.9619**	0.9071	0.8879	0.9613	**0.9511**	**0.9583**	**0.9127**	20
WNISM [9]	0.9370	0.9419	0.8109	0.8936	0.8600	0.8757	0.9212	0.8270	18
RR-SSIM [13]	**0.9555**	**0.9539**	**0.9493**	**0.8978**	**0.9642**	0.8692	0.9137	**0.9129**	36
Zhang *et al*. [10]	0.9134	0.9495	**0.9105**	**0.9294**	0.8417	0.9265	**0.9365**	0.8832	12
Ma *et al.* [15]	0.7945	0.8717	0.8042	**0.9100**	0.8619	0.9214	0.8866	0.8807	189
βW-SCM [11]	0.9495	0.9517	0.8535	0.8705	**0.9715**	**0.9371**	0.9258	0.8391	6
PSNR	0.9241	0.8628	0.8783	0.7698	**0.9853**	0.7829	0.8896	0.8749	L

Table 3: Experimental results of CC for the proposed method and the state of the art RR IQA methods and PSNR, evaluated by LIVE database.

Model/Distortion	JP2(1)	JP2(2)	JPEG(1)	JPEG(2)	Noise	Blur	FF	Overall	No. of scalars
RR-LBPS$_{P,R}^{u2}$	**0.9707**	**0.9669**	**0.9143**	**0.9752**	0.9632	**0.9650**	**0.9572**	**0.9141**	56
RR-LBPS$_{P,R}^{riu2}$	**0.9591**	**0.9628**	**0.9113**	0.9748	0.9638	**0.9594**	**0.9573**	**0.9082**	20
WNISM [9]	0.9339	0.9488	0.8278	0.9566	0.8769	0.8395	0.9230	0.8284	18
RR-SSIM [13]	**0.9597**	**0.9632**	**0.9448**	**0.9761**	**0.9772**	0.9154	**0.9315**	**0.9194**	36
Zhang *et al*. [10]	0.9087	0.9511	0.9094	**0.9777**	0.8623	0.9234	0.9234	0.8744	12
Ma *et al.* [15]	0.8065	0.8819	0.8180	0.9663	0.8769	0.9092	0.9178	0.8841	189
βW-SCM [11]	0.9514	0.9569	0.8673	0.9568	**0.9755**	**0.9454**	0.9243	0.8353	6
PSNR	0.9241	0.8628	0.8783	0.7698	**0.9853**	0.7829	0.8896	0.8749	L

Table 4: Experimental results of SROCC for the proposed method and the state of the art RR IQA methods and PSNR, evaluated by the CSIQ database.

Model/Database	CISQ	No. of scalars
RR-LBPS$_{P,R}^{u2}$	**0.8790**	56
RR-LBPS$_{P,R}^{riu2}$	**0.8730**	20
WNISM [9]	0.7431	18
RR-SSIM [13]	0.8527	36
Zhang *et al*. [10]	**0.8719**	12
Ma *et al.*[15]	0.8044	189
βW-SCM [11]	0.6389	6
PSNR	0.8058	L

Figure 3 shows the scatter plots after the nonlinear regression evaluated on LIVE and CSIQ database, where each point in the plots represents one test images. The vertical and horizontal axes are the perceived distortion and the objective score predicted by the proposed RR IQA methods respectively.

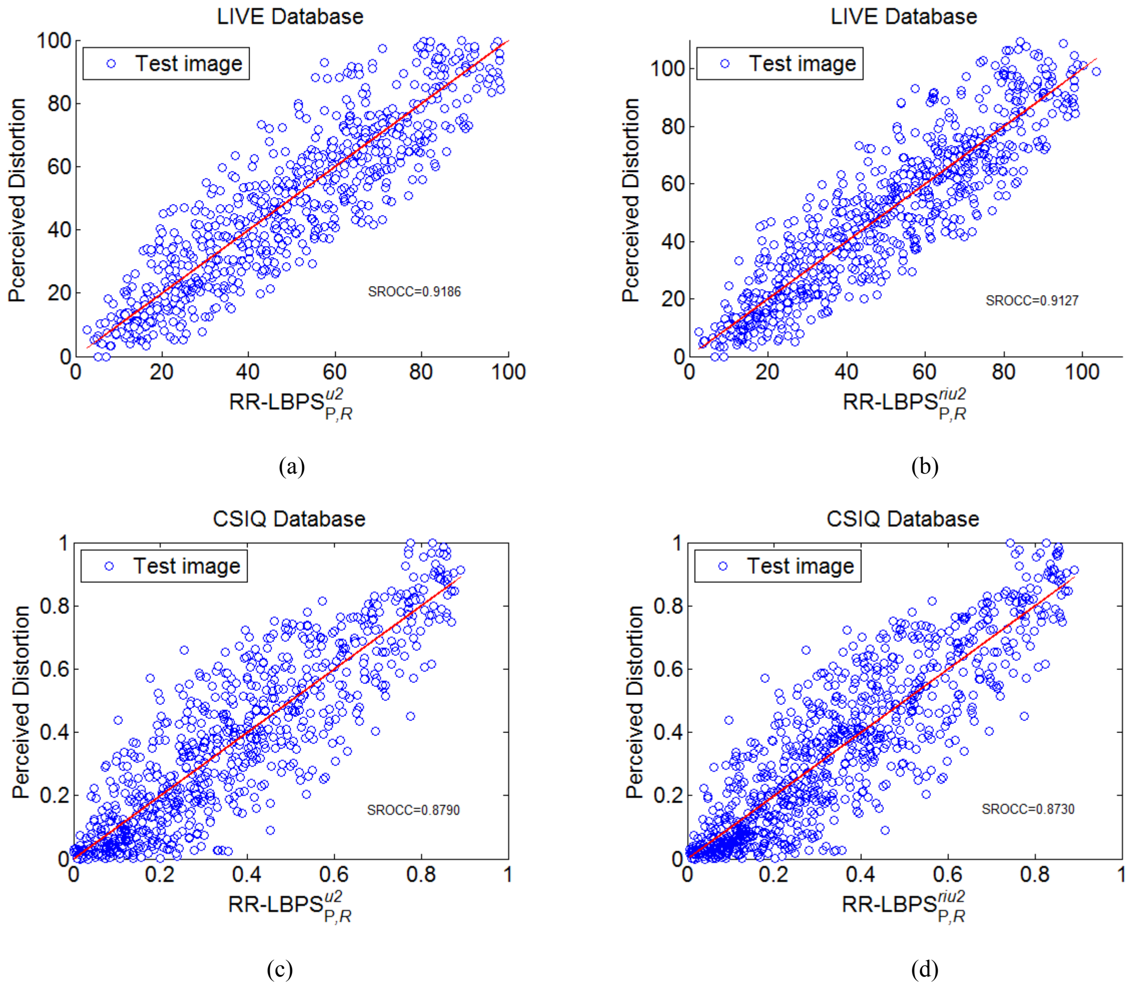

Figure 3 Scatter plots of the predicted quality distortion and perceived distortion for RR-LBPS$_{P,R}{}^{u2}$ and RR-LBPS$_{P,R}{}^{riu2}$ for LIVE database and CSIQ database respectively. (a) RR-LBPS$_{P,R}{}^{u2}$ for LIVE database. (b) RR-LBPS$_{P,R}{}^{riu2}$ for LIVE database. (c) RR-LBPS$_{P,R}{}^{u2}$ for CSIQ database. (d) RR-LBPS$_{P,R}{}^{riu2}$ for CSIQ database.

It can be observed from the experimental results that RR features from the histogram of LBP codes serve as a quite useful discriminant feature for quality evaluation with fairly low data rate. The proposed methods, both RR-LBPS$_{P,R}{}^{u2}$ and RR-LBPS$_{P,R}{}^{riu2}$, exhibit highly competitive performance in most cases concerning both the specific distortion types and the overall performance.

5. CONCLUSION

This paper presented a novel and concise RR IQA method. Local binary pattern is introduced as a similarity measure to develop a novel RR-IQA method for the first time. Experimental results on two large scale subject-rated image databases show that the proposed method exhibits good correlations with subjective evaluation over a wide variety of image distortions. The proposed method has the fair low RR data rate (at most 20 scalar features (with rotation invariance and uniform local binary pattern) and 56 scalar features (with uniform local binary pattern) per image in the implementation of this study). The proposed method is also applicable to no reference (NR) IQA and video quality assessment (VQA), which will be presented in our future work.

6. AKNOWLEDGEMENT

The authors thank members of the Fujita Laboratory for their valuable discussions. The authors also gratefully acknowledge the Venture Business Laboratory (VBL) of Gifu University for the support of this research work.

REFERENCES

[1] S. Daly, "The visible difference predictor: An algorithm for the assessment of image fidelity," Proc. SPIE, vol. 1616, pp. 2–15, 1992.

[2] E. C. Larson and D. M. Chandler, "Most apparent distortion: Full-reference image quality assessment and the role of strategy", J. Electron. Imaging 19, 011006 , 2010.

[3] D. M. Chandler and S. S. Hemami, "VSNR: A wavelet-based visual signal-to-noise ratio for natural images," IEEE Trans. Image Process. vol. 16, no. 9, pp. 2284-2298, 2007.

[4] Z. Wang, A. C. Bovik, H. R. Sheikh, and E. P. Simoncelli, "Image quality assessment: From error measurement to structural similarity," IEEE Trans. Image Processing, vol. 13, no. 4, pp. 600–612, 2004.

[5] Min Zhang, Xuanqin Mou, Lei Zhang, "Non-Shift Edge based Ratio (NSER): An Image Quality Assessment Metric based on Early Vision Features". IEEE Signal Processing Letters, 18(5): 315-318, 2011.

[6] H. R. Sheikh, A. C. Bovik, and G. de Veciana, "An information fidelity criterion for image quality assessment using natural scene statistics," IEEE Trans. Image Process., vol. 14, no. 12, pp. 2117–2128, 2005.

[7] H.R. Sheikh and A.C. Bovik, "Image information and visual quality," IEEE Trans. Image Process., vol.15, no.2, pp. 430- 444, 2006.

[8] VQEG. Final report from the video quality experts group on the validation of objective models of video quality assessment," Apr. 2000. http://www.vqeg.org/.

[9] Z. Wang, G. Wu, H. R. Sheikh, E. P. Simoncelli, E. H. Yang, and A. C. Bovik, "Quality-aware images," IEEE Trans. Image Process., vol. 15, no. 5, pp. 1680–1689, 2006.

[10] M. Zhang, W. Xue, and X. Mou, "Reduced reference image quality assessment based on statistics of edge," vol. 7876, no. 1. San Francisco Airport, California, USA: SPIE, p. 78761, 2011.

[11] W. Xue and X. Mou, "Reduced reference image quality assessment based on weibull statistics," in Second International Workshop on Quality of Multimedia Experience (QoMEX), pp. 1–6, 2010.

[12] X. Gao, W. Lu, D. Tao, and X. Li, "Image quality assessment based on multiscale geometric analysis," IEEE Trans. Image Process., vol. 18,no. 7, pp. 1409–1423, 2009.

[13] A. Rehman and Z. Wang, "Reduced-Reference Image Quality Assessment by Structural Similarity Estimation", IEEE Trans. Image Process., vol. 21, pp. 3378-3389, 2012.

[14] R. Soundararajan and A. C. Bovik, "RRED Indices: Reduced Reference Entropic Differencing for Image Quality Assessment," IEEE Transactions on Image Processing, vol. 21, no. 2, pp. 517-526, 2012.

[15] L. Ma, S. Li, F. Zhang, and K. N. Ngan, "Reduced-reference image quality assessment using reorganized dct-based image representation," IEEE Transactions on Multimedia, vol. 13, no. 4, pp. 824–829, 2011.

[16] T. Ojala, M. Pietikainen, and T. Maenpaa, "Multiresolution gray-scale and rotation invariant texture classification with local binary patterns", IEEE Transactions on Pattern Analysis and Machine Intelligence, 24(7):971-987, 2002.

[17] X. Tan, and B. Triggs, "Enhanced Local Texture Feature Sets for Face Recognition Under Difficult Lighting Conditions," in Proc. International Workshop on Analysis and Modeling of Faces and Gestures, pp.168-182, 2007.

[18] H. R. Sheikh, Z. Wang, L. Cormack, and A. C. Bovik. (2005) Live Image Quality Assessment Database Release 2. [Online]. Available: http://live.ece.utexas.edu/research/quality.

[19] E. C. Larson and D. M. Chandler, "Categorical image quality (csiq) database," Online, http://vision.okstate.edu/csiq/.

[20] Z. H. Guo, L. Zhang and D. Zhang, "A Completed Modeling of Local Binary Pattern Operator for Texture Classification," IEEE Transactions on Image Processing, vol.19, no.6, pp.1657-1663, 2010.